

# The BARC biosensor applied to the detection of biological warfare agents

R.L. Edelstein <sup>a,\*</sup>, C.R. Tamanaha <sup>b</sup>, P.E. Sheehan <sup>b</sup>, M.M. Miller <sup>b</sup>, D.R. Baselt <sup>b,1</sup>,  
L.J. Whitman <sup>b</sup>, R.J. Colton <sup>b</sup>

<sup>a</sup> *Geo-Centers, Inc., PO Box 441340, Fort Washington, MD 20749-1340, USA*

<sup>b</sup> *Naval Research Laboratory, 4555 Overlook Ave., SW, Washington, DC 20375, USA*

Received 1 July 1999; received in revised form 12 September 1999; accepted 17 September 1999

## Abstract

The Bead ARray Counter (BARC) is a multi-analyte biosensor that uses DNA hybridization, magnetic microbeads, and giant magnetoresistive (GMR) sensors to detect and identify biological warfare agents. The current prototype is a table-top instrument consisting of a microfabricated chip (solid substrate) with an array of GMR sensors, a chip carrier board with electronics for lock-in detection, a fluidics cell and cartridge, and an electromagnet. DNA probes are patterned onto the solid substrate chip directly above the GMR sensors, and sample analyte containing complementary DNA hybridizes with the probes on the surface. Labeled, micron-sized magnetic beads are then injected that specifically bind to the sample DNA. A magnetic field is applied, removing any beads that are not specifically bound to the surface. The beads remaining on the surface are detected by the GMR sensors, and the intensity and location of the signal indicate the concentration and identity of pathogens present in the sample. The current BARC chip contains a 64-element sensor array, however, with recent advances in magnetoresistive technology, chips with millions of these GMR sensors will soon be commercially available, allowing simultaneous detection of thousands of analytes. Because each GMR sensor is capable of detecting a single magnetic bead, in theory, the BARC biosensor should be able to detect the presence of a single analyte molecule. © 2000 Elsevier Science S.A. All rights reserved.

*Keywords:* Biosensor; Magnetoresistive technology; DNA patterning; DNA hybridization; Magnetic beads; Fluidics

## 1. Introduction

The threat of biological warfare is an increasing concern. Advances in microbiology and genetic engineering have made it possible to create extremely dangerous microorganisms. Because methods for detection of these agents and treatments for infection are currently limited, the development of highly sensitive sensors for early detection of biological warfare agents is crucial.

There are many ways to detect biological molecules, however, most biosensors rely on specific molecular recognition events such as antibody–antigen, DNA–DNA, or other ligand–receptor interactions between molecules. These recognition events are usually detected

indirectly by a variety of labeling techniques that employ radioactive, enzymatic, or fluorescent labels, followed by scintillation counting, recording color changes, or monitoring light emission. Each method has its advantages and limitations. For example, radioimmunoassays, once an industry standard, require expensive instrumentation and the handling and disposal of radioactive wastes. Recently, several methods have been developed for direct measurement of DNA hybridization without the need for labeling: for instance, DNA hybridization has been detected directly using evanescent wave sensors (Watts et al., 1995; Abel et al., 1996), a quartz crystal microbalance (Okahata et al., 1992), and optical interferometric measurements of porous silicon (Lin et al., 1997). Other important advances have been in the area of DNA array technology. Methods have been developed for in situ synthesis of high density DNA arrays on glass and silicon substrates using photolithography (Fodor et al., 1991; Chee et al.,

\* Corresponding author.

<sup>1</sup> Present address. Graviton, Inc., 11588 Sorrento Valley Road Suite 16, San Diego, CA 92121, USA.

1996) and semiconductor photoresists (McGall et al., 1996). Devices are also being built that can deliver pre-synthesized oligonucleotides in small, well-defined spots onto solid substrates using ink-jet delivery (Blanchard et al., 1996) and micro-contact pen (also called pin, tip, or quill) spotting (Graves et al., 1998; Bowtell, 1999). Array technology is a significant advancement for biosensor development since it makes multianalyte analysis feasible. However, current readers and detectors for DNA array chips typically use radioisotope or fluorescence measurements, requiring relatively large and expensive instrumentation.

We are developing a revolutionary bioassay that uses DNA arrays, magnetic microbeads, and GMR sensors to detect biomolecules. A significant advantage of our sensor over more traditional detection methods is that we apply a magnetic field gradient to test the bonding between interacting molecular species. The applied force discriminates between species that are specifically and non-specifically bound, resulting in increased selectivity (i.e. lower false positives and negatives) and increased sensitivity (i.e. lower backgrounds).

### 1.1. BARC biosensor overview

Development of the BARC biosensor has been enabled by recent advances in two areas: magnetoresistive materials and magnetic microbeads. Over the past few years, magnetoresistive materials have been discovered which allow the microfabrication of magnetic field sensors with high sensitivity and micrometer-scale size. These giant magnetoresistive (GMR) materials are typically thin-film metal multilayers, the resistance of which changes in response to magnetic fields. By passing a current through a strip of GMR material and measuring its resistance, local magnetic fields can be measured. The BARC sensor uses this technology to detect the presence of magnetic microbeads, which a number of companies have independently developed for biological separations and purification. The beads are typically paramagnetic particles (they are only magnetic in the presence of a magnetic field), containing an iron oxide core and a polymer coating onto which proteins or antibodies are attached, and we are evaluating several types for use in the BARC biosensor.

The prototype BARC instrument, currently under development, is a table-top instrument consisting of a microfabricated chip (solid substrate) with an array of GMR sensors, a chip carrier board with electronics for lock-in detection, a fluidics cell and cartridge, and an electromagnet (Fig. 1) (Baselt et al., 1998). Thiolated DNA probes will be patterned onto a gold layer on the solid substrate chip directly above the GMR sensors using micro-contact pen spotting. Prior to analysis with BARC, sample DNA will be biotin labeled during PCR amplification. When a sample is injected into the instru-

ment, it will hybridize with probes on the chip surface if the complementary sequence is present. Streptavidin-labeled paramagnetic beads will then be added that specifically bind to the biotinylated sample DNA on the chip surface. Any beads that are not specifically bound will be removed by applying a magnetic field gradient with the electromagnet. The GMR sensors will detect the beads remaining on the surface, and the intensity and location of the signal will indicate the concentration and identity of pathogens present in the sample (Fig. 2). In this manuscript, we describe our current progress in the development of each of the following BARC components: DNA patterning and the hybridization assay; the GMR sensor chip, magnetics, and signal detection; and fluidics.

## 2. Results and discussion

### 2.1. DNA patterning and hybridization assay

Although BARC will be capable of detecting a wide variety of molecular recognition reactions, we are initially using DNA hybridization to detect the following biological warfare agents: *Bacillus anthracis*, *Yersinia pestis*, *Brucella suis*, *Francisella tularensis*, *Vibrio cholerae*, *Clostridium botulinum*, *Campylobacter jejuni*, and Vaccinia virus. In order to avoid expending our limited supply of sensor chips, we have been developing the DNA immobilization chemistry and optimizing the

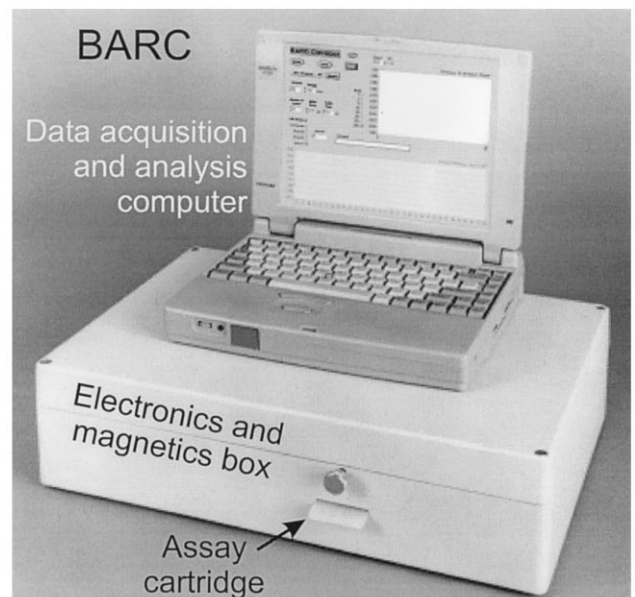


Fig. 1. Photograph of the table-top BARC prototype. The BARC chip and fluidics are contained in the assay cartridge, the electromagnet assembly and electronics in the electronics and magnetics box. A portable computer is used for data acquisition and analysis via a connection with the serial port.

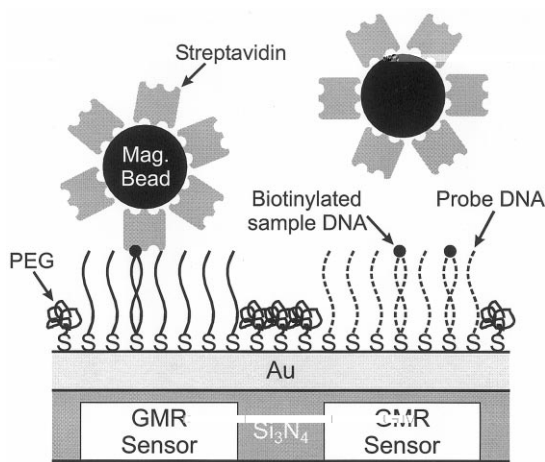


Fig. 2. Schematic diagram of the BARC chip surface chemistry and hybridization assay. Thiolated DNA probes are patterned onto a gold layer directly above the GMR sensors on the BARC chip. Biotinylated sample DNA is then added and hybridizes with the DNA probes on the surface when the complementary sequence is present. Unbound sample DNA is washed away. Streptavidin coated magnetic beads are injected over the chip surface, binding to biotinylated sample DNA hybridized on the BARC chip. Beads that are not specifically bound are removed by applying a magnetic field. Bound beads are detected by the GMR sensors.

sium phosphate buffer, pH 7), thiolated at the 3'-end, are spotted onto the gold surface with Rapidograph<sup>®</sup> pens. To enhance hybridization, we use DNA oligomers that contain a 3-carbon spacer and six extra nucleotides between the 3'-thiol and the probe sequence. These spacers are used to reduce steric hindrance caused by oligonucleotide packing at the substrate surface that makes bases near the surface less accessible for hybridization. It has previously been shown that hybridization efficiency can be increased two orders of magnitude by including such spacer arms (Southern et al., 1999). Immediately after arraying, the surfaces are put in a humid chamber at 37°C for 6–24 h. To prevent nonspecific adhesion of sample DNA and of the magnetic beads to the unmodified areas of the gold surface, the arrayed surfaces are also treated with thiolated PEG (*O*-(2-mercaptoethyl)-*o'*-methyl-polyethylene glycol 5000, 10 mg/ml in deionized water for 1 h at room temperature).

### 2.1.2. DNA hybridization

The arrayed surfaces are prepared for hybridization by incubation in 2X SSC buffer (0.3 M NaCl, 30 mM sodium citrate, pH 7.0) containing 0.25% sodium dodecyl sulfate (SDS) for at least 0.5 h. Biotinylated sample DNA is then hybridized to the arrays by submerging the arrayed surface in sample DNA solution (0.10 pM–1.0  $\mu$ M in 2X SSC buffer containing 0.25% SDS) for 3 h at room temperature (note that we recently obtained similar results when the hybridization time is reduced to 0.5 h.). The surfaces are then washed twice with 2  $\times$  SSC buffer containing 0.25% SDS, followed by another two washes with 1  $\times$  SSC buffer containing 0.125% SDS. Each wash is performed by immersing the surfaces into the buffer solution for 5 min while shaking. Magnetic beads coated with streptavidin (Seradyne's 0.7  $\mu$ m Sera-Mag<sup>™</sup> Streptavidin Magnetic Microparticles) are then added and allowed to settle onto the surface. We have also used Dynal's 2.8  $\mu$ m M-280 Streptavidin Dynabeads<sup>®</sup>, but these resulted in higher non-specific background adhesion. A permanent magnet is placed over the surface to remove non-specifically bound beads. Images are captured before and after the magnet is applied using an optical microscope and a video image frame-grabber. The numbers of beads on the arrayed areas are compared using image analysis software.

Fig. 3 shows the optical micrograph results of one such hybridization experiment. The gold substrates used in this experiment were arrayed with a DNA probe for *B. anthracis* lethal factor (270  $\mu$ m<sup>97</sup>(to)-43s74((2

beads. The bottom panels show specific hybridization of a single-stranded complementary oligonucleotide (10 nM) to the arrayed area on the substrate.

The multi-analyte capability of the assay is illustrated in Fig. 4. In this case, three different probes were arrayed across the gold substrates. A thiolated and biotinylated probe was spotted in the top row of the substrate as a positive control and as an orientation marker. The ALF probe is in the second row, and the *C. botulinum* neurotoxin A (BA) probe is in the third row. The image on the left shows the optical micrograph results after single-stranded DNA complementary to the ALF probe was hybridized to the surface, streptavidin magnetic beads added, and a magnetic field applied to remove nonspecifically bound beads. The image on the right shows the results of hybridization with DNA complementary to the BA probe. These results demonstrate the high specificity of the assay and the low cross-reactivity of the probes with non-complementary DNA.

We have also optically examined the sensitivity of the assay using a 3-h hybridization time (Fig. 5). Different concentrations of a single-stranded oligomer complementary to the BA probe were hybridized to gold surfaces patterned with the BA probe and a biotinylated control probe. The numbers of beads remaining

on the surface after application of the magnet were compared for the different concentrations and were normalized using the number of beads bound to the biotinylated control probe. We are able to detect DNA at 100 fM concentrations using the optical assay, with the sensor saturated above 1 nM concentrations. 100 pM noncomplementary DNA gives a background signal (normalized number of beads) of 0.08 (data not shown). We expect the addition of the fluidics and GMR sensor signal detection to greatly improve assay sensitivity. Varying the hybridization times should also increase the sensitivity range.

## 2.2. GMR sensor chip, magnetics, and signal detection

### 2.2.1. GMR sensor chip

We currently use a second generation prototype BARC GMR sensor chip, custom-fabricated by Non-volatile Electronics (Eden Prairie, MN) according to our designs. Previously, we described in detail the fabrication and detection response of our first generation  $2.5 \times 2.5$  mm prototype chip (Baselt et al., 1998). Our second generation 64-element chips were designed with the optimal GMR sensor geometry ( $80 \times 5$   $\mu\text{m}$  sensor strips), positioned in eight clusters of eight sensor strips onto which DNA probes will be patterned, as shown in

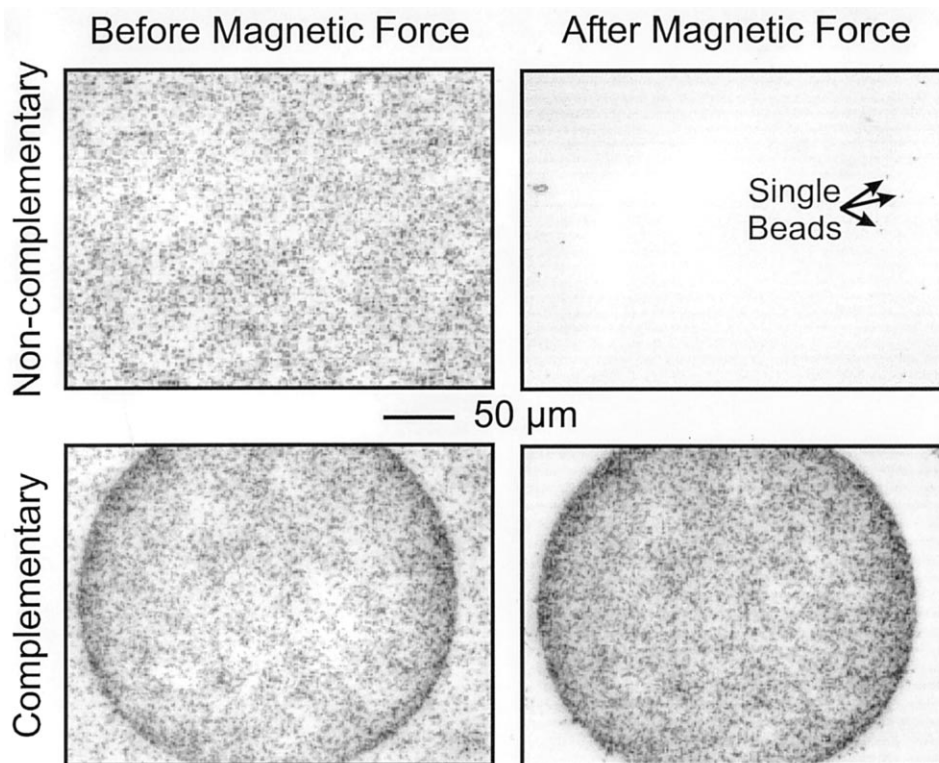


Fig. 3. Optical micrographs of gold-coated silicon substrates showing a DNA hybridization assay before and after application of a magnetic field. The gold substrates contain  $270 \mu\text{m}$ -diameter spots of *Bacillus anthracis* lethal factor probe. The top panels show the results for a substrate exposed to non-complementary biotinylated DNA followed by addition of streptavidin magnetic beads. The bottom panels show the specific hybridization of complementary biotinylated DNA.

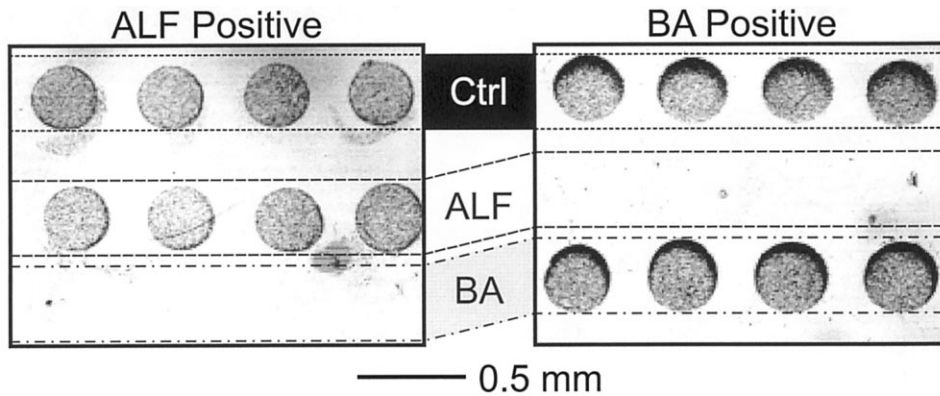


Fig. 4. Optical micrograph showing 2-analyte assay. A thiolated and biotinylated DNA probe was spotted in the top row of the gold substrate as a positive control, Bacillus anthraxis lethal factor (ALF) probe in the second row, and a DNA probe for *C. botulinum* neurotoxin A (BA) in the third row. The left panel shows the results after biotinylated DNA complementary to the ALF probe was hybridized to the surface, streptavidin magnetic beads added, and a magnetic field applied to remove the non-specifically bound beads. The right panel shows the analogous results following hybridization with DNA complementary to the BA probe.

Fig. 6. The chip contains these clusters of sensors in order to optimize assay sensitivity. GMR sensor sensitivity increases with decreasing surface area of the sensor, however, the chemical sensitivity, or number of analyte molecules that can hybridize to the surface, increases with increasing surface area. Therefore, a cluster of small sensors allows both chemical and instrument sensitivity. Each sensor strip is capable of single bead detection, similar to the first prototype BARC chips (Baselt et al., 1998). The strips are connected to aluminum leads, designed to minimize resistance, which terminate in wirebond pads in the corners of each chip. To facilitate connection with the electronics, the BARC chip is wire-bonded to a chip carrier board. A thin layer ( $\sim 500$  Å) of gold can be coated over the entire chip, except on the wire-bond pads, without interfering with bead detection. The chips are  $5 \times 5$  mm and were designed to allow integration with fluidics, as described below.

### 2.2.2. Electromagnet

Given the special magnetic field requirements for BARC, we have custom designed an electromagnet that integrates with the BARC chip and fluidics. The magnetic field requirements and resulting assembly are displayed in Fig. 7. If the magnetoresistive sensors lie in the XY plane and current flows through them in the X direction, the GMR sensors only detect the X component of the magnetic field. Therefore, to detect paramagnetic beads on top of a GMR strip, a *uniform* magnetic field must be generated in the Z direction (Baselt et al., 1998). Our custom-made electromagnet produces fields that are perpendicular to the Z axis to within  $0.5^\circ$ . However, separating the nonspecifically bound magnetic beads from the specifically bound beads requires a *non-uniform* large field gradient; the transition from uniform to non-uniform magnetic field

is accomplished by moving a portion of the electromagnetic core closer to the chip with the plunger.

### 2.2.3. Signal detection

We have previously shown that a BARC GMR sensor strip can detect the presence of a single magnetic bead by incorporating two GMR elements (one signal and one reference) into a Wheatstone bridge, applying an AC magnetizing-field, and detecting the resistance change with a lock-in amplifier (Baselt et al., 1998). We have since expedited detection by adding four separate lock-in detectors as well as off-board switching circuitry and incorporated the custom-built electromagnet and fluidics cell. All the required electronics have been built

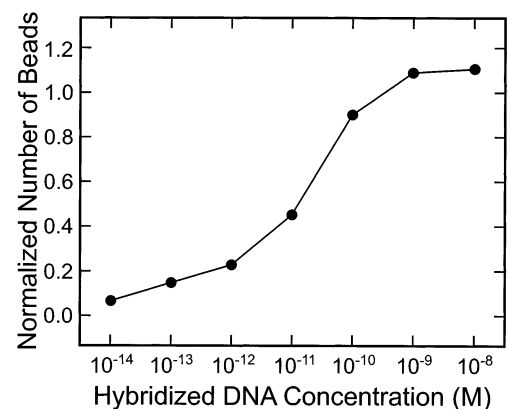


Fig. 5. Optical assay sensitivity. Different concentrations (0.1 pM–10.0 nM) of single-stranded DNA complementary to the BA probe were hybridized to gold surfaces patterned with both the BA probe and a biotinylated control probe. The number of beads after application of the magnet was counted (using an optical microscope and image analysis software) and normalized against the number of beads bound to the control probe for each concentration. The normalized number of beads shown are the ratios of the average number of beads remaining on the surface (after the magnetic field was applied) for three BA spots and three control probe spots.

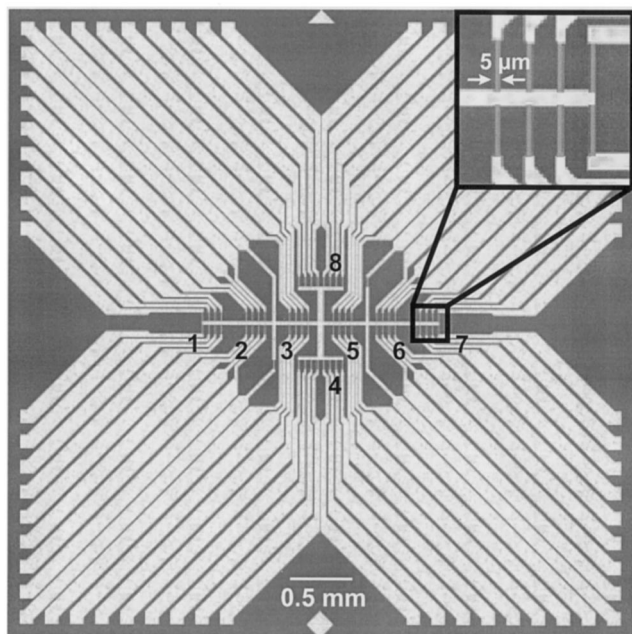


Fig. 6. Optical micrograph of the prototype 64-element BARC chip showing eight clusters of eight sensor regions. A DNA probe will be spotted above each cluster. Inset: Enlargement of a single cluster of eight GMR sensor strips.

and are currently being calibrated and optimized. We have now shown that the prototype is capable of detecting Dynabeads<sup>®</sup> M-280 on the surface at relatively low concentrations (less than a full bead per sensor). To do this, the signal from each sensor is measured 64 times and the results averaged. Measurement of the signal from all 64 sensors currently takes 5 min, with the majority of this time used for lock-in settling time. In Fig. 8, the signal from a number of elements is shown. On the left is the signal from a 16-element section of the array recorded after the beads in an injected solution have been allowed to settle, leaving 360 beads/mm<sup>2</sup> randomly distributed over the detector. The signal for each sensor varies depending on whether a bead is directly on the sensor (elements two and 15), off the sensor (elements 11 and 14), or near the edge of the sensor (all others). Note that averaging the signal from multiple sensors will eliminate this variation. For comparison, the results for the same experiment when no beads are injected are shown on the right, clearly indicating that there is no appreciable signal without the presence of beads.

### 2.3. Fluidics system to interface with the BARC chip

A carefully designed fluidics system is required to ensure uniform sample and bead flow over the sensor

#### 2.3.1. Detector flow cell

The uniformity of the microbead dispersion across the GMR sensors has been assessed with fluid flow models. This is critical for assay-to-assay consistency because if a certain sensor were to receive significantly more beads than another, it would register a false positive. Numerical finite-element analysis simulations indicate that the simplest effective channel geometry is that of a diffuser (Fig. 9a). This feature has been incorporated in the design of the prototype fluidics cell (Fig. 9b). For investigative purposes, the prototype fluidics cells, with an internal volume of 1.5 μl, are made from quartz by high precision mechanical diamond tool machining (Mindrum Precision). Tubing is attached to the fluidics cell with 28-gauge (0.305 mm ID) polyimide tubing connectors. With quartz, we gain the benefit of reusability and a simple attachment of the cells to the BARC chip using UV curing epoxy (Norland optical adhesive # 72, Norland Products). We

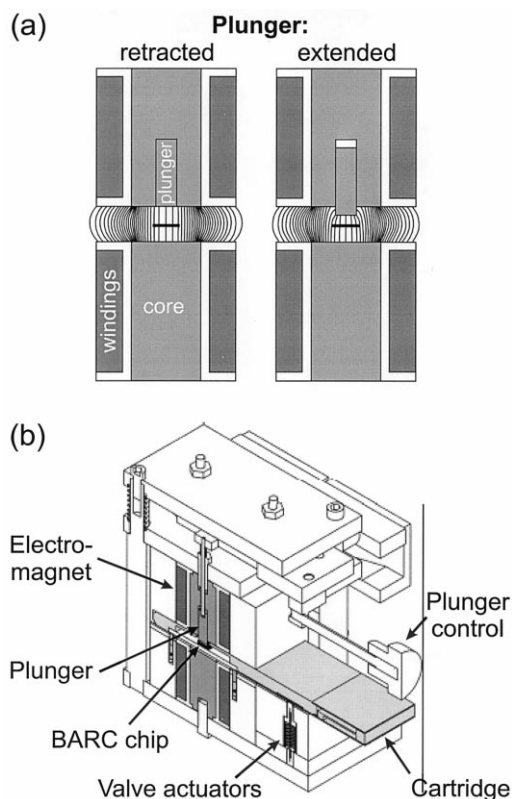


Fig. 7. Electromagnet core and assembly. (a) The magnetic field lines for the two electromagnet configurations: when the plunger is retracted, there is a homogeneous field between the two poles. At 200 Hz AC, the electromagnet will produce an alternating field of 100 G RMS. When the plunger is extended, the field is no longer homogeneous, producing a 2250 G/cm field gradient for removal of non-specifically bound beads. (b) Cutaway schematic of the complete electromagnet assembly. When a cartridge is inserted, a plunger control is used both to lock the cartridge in place, making solid connections to the valve actuators and contact pins, and to raise and lower the core plunger as described above. For scale, the length of the cartridge is 10 cm.

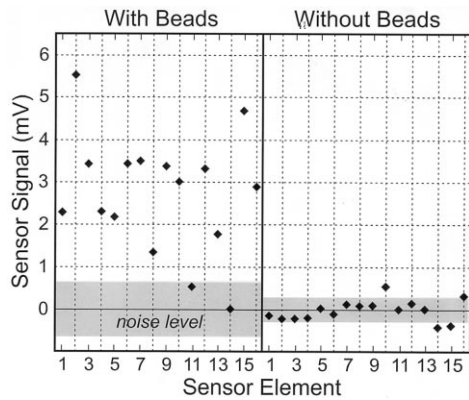


Fig. 8. Detection of magnetic beads with the BARC prototype. The graphs show the signals from 16 of the 64-sensor elements with and without adsorbed beads. The graph on the left shows that beads are easily detected. The signal due to a single bead varies from strip to strip depending on whether the bead is directly on top of the sensor (elements two and 15), not present (11 and 14), or near the edge of the sensor (all others). The noise level is determined by measuring the signal before beads are injected and after they are washed off and is slightly higher with beads than without beads because the wash is not 100% efficient.

have found that the epoxy is sufficiently viscous to wick between the cell and chip surface without entering the fluidics chamber enclosing the GMR sensors despite the 1  $\mu\text{m}$  high traces. In addition, the epoxy does not affect the flow of microbeads at the periphery interface of the fluidics chamber. Eventually, thermoplastic molding processes will replace quartz machining to assure repro-

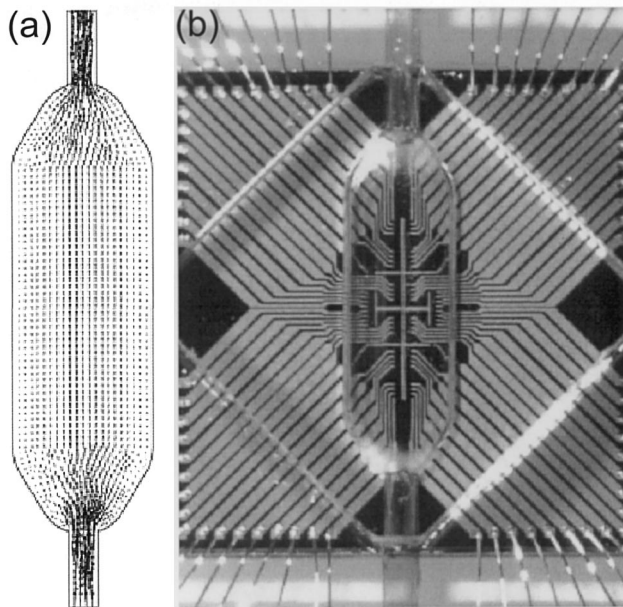


Fig. 9. Detector flow cell. (a) Simulation of fluid flow in a diffuser channel positioned over the 64 GMR sensors in the center of the BARC chip. (b) Optical micrograph of the quartz cell when mounted on an actual BARC chip.

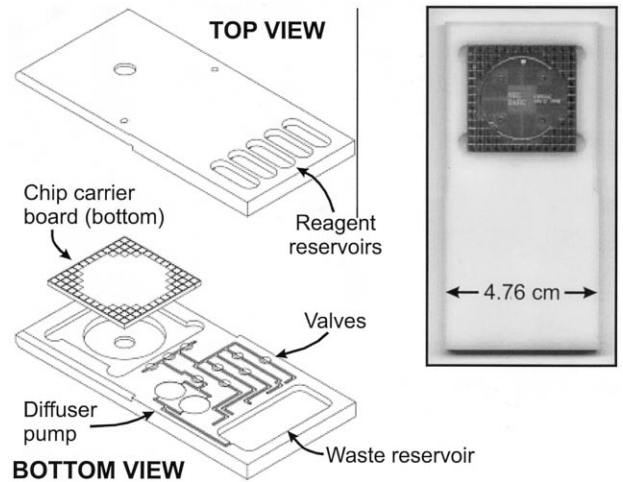


Fig. 10. Design of the plastic fluidics cartridge ( $4.76 \times 10.16$  cm). The top view shows the planned reagent reservoirs. The bottom view shows the mount for the chip carrier board and where the pumps and valves will be to direct the flow of reagents through the liquid cell. A photograph of a prototype cartridge (with a chip but without fluidics) is also shown.

ducibility of fine fluidics channel detail, high production volume, and low material cost.

### 2.3.2. Fluidics cartridge

As part of the integrated sensor fluidics system, we are currently developing thermoplastic-molded, micron-scale channels, negative displacement pumps, membrane valves, and reservoirs. These components are being incorporated into disposable fluidics cartridges that will ultimately each contain a BARC chip mounted on a printed circuit carrier board as illustrated in Fig. 10. Because each experiment will be performed in its own cartridge, and the fluids will be completely contained within the cartridge, the disposable fluidics will serve to prevent cross-contamination between assays.

Although similar fluidics systems have been developed in the past, BARC presents a unique set of challenges. The high sensitivity of the assay and the use of magnetic particles place strict limits on the materials and component designs that can be used. Furthermore, the magnetic beads that we are using in our assay are dense and tend to settle out of solution rapidly. Piezoelectric mixing elements will be used to keep beads suspended in solution. We plan to use a pumping mechanism based on the valveless diffuser pump (Stemme and Stemme, 1993). This unique pump is ideal for thermoplastic molding because of its planar, compact shape. The direction-dependent flow resistance of the pair of diffuser/nozzle elements in the pump creates a unidirectional fluid flow that makes check valves unnecessary. This is advantageous since particles such as microbeads could render mechanical check valves inoperative.

Cartridge fluidics is currently being prototyped by conventional milling of plastic substrates, followed by press-molding of diffuser-nozzle elements with a metal mold pin. A prototype pump we have made in this fashion has achieved  $\sim 150 \mu\text{l}/\text{min}$  flow rates with an actuation frequency of  $\sim 700 \text{ Hz}$ . Chemical modification of the fluidic channel surfaces will be done to prevent adhesion and loss of biomaterial onto the channel walls. Once we have optimized the layout and functionality of the fluidics system, we will mass-produce the cartridges by thermoplastic injection- and press-molding methods.

### 2.3.3. Actuators

Actuation of the valves and pumps to dispense fluids retained in the cartridge will be entirely automated. The actuators will be a separate unit located in the BARC instrument enclosure and will interface with the 4.76 cm wide cartridge via a kinematic mount when the cartridge is inserted into the instrument. Hence, the multi-use cartridge will be an inexpensive, disposable component of the system. The layout of the cartridge fluidics and location of the GMR sensor array chip limits the pump and valve actuator block to a  $2.54 \times 5.08 \times 2.54 \text{ cm}$  volume to be located below the cartridge during interfacing.

Our pumps require actuators able to withstand several Newtons of blocked force while providing  $> 100 \mu\text{m}$  of linear motion. A piezoelectric stack was determined best able to address this problem. We have designed a titanium mechanical amplifier incorporating a monolithic flexure hinged class three lever system to extend the linear motion of the piezoelectric stacks. Finally, to control the flow of fluid at channel junctions, clog-proof membrane valves are being developed by using off-cartridge shape memory alloy actuators to ‘pinch off’ particular channels. Because of the close proximity of the channels and the use of magnetic beads, the valve actuators have been designed with non-magnetic components.

## 3. Conclusions and future directions

We have shown here our results and progress in the development of each of the components for the BARC biosensor. The current prototype is a table-top instrument designed to detect several biological warfare agents simultaneously. The total active area of our 64-element GMR arrays is limited because each sensor has a separate connection to the off-chip circuitry. To increase the active area of the chip and thereby achieve the full multi-analyte potential of BARC, we will eventually need to add switching circuitry to the chip so that multiple sensors can share a single off-chip connection. Fortunately, the technology to fabricate million-sensor

magnetoresistive arrays with on-chip addressing is currently being developed for use in nonvolatile magnetoresistive memory (MRAM) (Daughton, 1992). Such devices could be adapted for BARC, with each storage bit acting as a single BARC sensor element as illustrated in the cartoon in Fig. 11. It is noteworthy that the design criteria for BARC chips are actually less stringent than those for MRAM—longer access times, larger sensors, and lower sensitivity are all permissible. Commercial MRAM fabrication of  $1 \times 1 \text{ cm}$  chips containing one million  $0.4 \times 1.2 \mu\text{m}$  sensors is expected to begin in late 1999. Because the sensors in this chip are smaller than our magnetic particles, a BARC sensor incorporating such an array would effectively create a  $1 \mu\text{m}$ -resolution image of the magnetic particle distribution on its surface; the image acquisition would take 2–3 s. Such a chip would have a usable area equivalent to 4000 of our present 64-element arrays. The huge active area of an MRAM-type chip could, at one extreme, be divided among 1000 different analytes (using four probes per analyte). At the other extreme, the entire chip could be devoted to a single analyte, resulting in very high sensitivity.

## Acknowledgements

This work was supported in part by the Defense Advanced Research Projects Agency. CRT is grateful for an American Society for Engineering Education postdoctoral fellowship, and PES for a National Research Council postdoctoral fellowship. We would like to thank O. Millard for her work on the optical assay

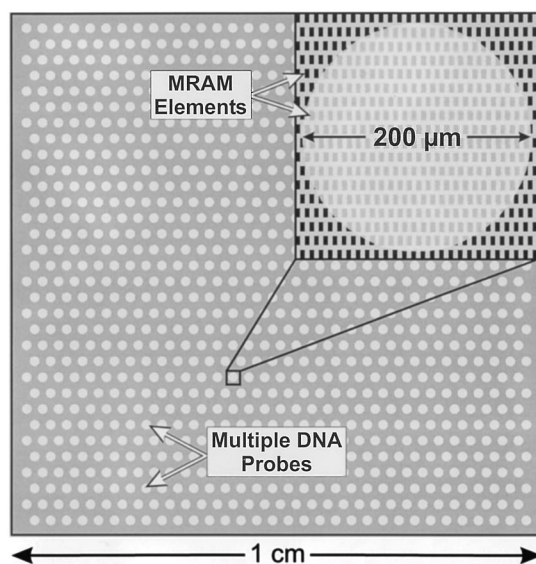


Fig. 11. Cartoon of how the BARC sensor concept might be integrated with an MRAM-type GMR array. Each  $200 \mu\text{m}$ -diameter spot of DNA probe would cover hundreds of MRAM elements for a high sensitivity,  $\sim 1000$  analyte biosensor.

and patterning, K. Lee for technical assistance on the electronics, and G. Long and C. Drombetta from NMRI for helpful discussions.

## References

- Abel, A.P., Weller, M.G., Duveneck, G.L., Ehrat, M., Widmer, H.M., 1996. Fiber-optic evanescent wave biosensor for the detection of oligonucleotides. *Anal. Chem.* 68, 2905–2912.
- Baselt, D.R., Lee, G.U., Natesan, M., Metzger, S.W., Sheehan, P.E., Colton, R.J., 1998. A biosensor based on magnetoresistance technology. *Biosens. Bioelectron.* 13, 731–739.
- Blanchard, A.P., Kaiser, R.J., Hood, L.E., 1996. Synthetic DNA arrays. *Biosens. Bioelectron.* 11, 687–690.
- Bowtell, D.D.L., 1999. Options available—from start to finish—for obtaining expression data by microarray. *Nature Genet. Suppl.* 21, 25–32.
- Chee, M., Yang, R., Hubbell, E., Berno, A., Huang, X.C., Stern, D., Winkler, J., Lockhart, D.J., Morris, M.S., Fodor, S.P.A., 1996. Accessing genetic information with high-density DNA arrays. *Science* 274, 610–614.
- Daughton, J.M., 1992. Magnetoresistive memory technology. *Thin Solid Films* 216, 162–168.
- Fodor, S.P.A., Read, J.L., Pirrung, M.C., Stryer, L., Lu, A.T., Solas, D., 1991. Light-directed, spacially addressable parallel chemical synthesis. *Science* 251, 767–773.
- Graves, D.J., Su, H.-J., McKenzie, S.E., Surrey, S., Fortina, P., 1998. System for preparing microhybridization arrays on glass slides. *Anal. Chem.* 70, 5085–5092.
- Herne, T.M., Tarlov, M.J., 1997. Characterization of DNA probes immobilized on gold surfaces. *J. Am. Chem. Soc.* 119, 8916–8920.
- Lin, V.S.-Y., Motesharei, K., Dancil, K.-P.S., Sailor, M.J., Ghadiri, M.R., 1997. A porous silicon-based optical interferometric biosensor. *Science* 278, 840–843.
- McGall, G., Labadie, J., Brock, P., Wallraff, G., Nguyen, T., Hinsberg, W., 1996. Light-directed synthesis of high-density oligonucleotide arrays using semiconductor photoresists. *Proc. Natl. Acad. Sci. USA* 93, 13555–13560.
- Okahata, Y., Matsunobu, Y., Ijiri, K., Mukae, M., Murakami, A., Makino, K., 1992. Hybridization of nucleic acids immobilized on a quartz crystal microbalance. *J. Am. Chem. Soc.* 114, 8299–8300.
- Southern, E., Mir, K., Shchepinov, M., 1999. Molecular interactions on microarrays. *Nat. Genet. Suppl.* 21, 5–9.
- Stemme, E., Stemme, G., 1993. A valveless diffuser/nozzle-based fluid pump. *Sens. Actuators A* 39, 159–167.
- Watts, H.J., Yeung, D., Parkes, H., 1995. Real-time detection and quantification of DNA hybridization by an optical biosensor. *Anal. Chem.* 67, 4283–4289.